The Fate of Star Clusters near the Galactic Center. I. Analytic Considerations

McMillan, S.L.W.; Portegies Zwart, S.F.

Published in:
Astrophysical Journal

DOI:
10.1086/377577

The Astrophysical Journal, 596:314–322, 2003 October 10

THE FATE OF STAR CLUSTERS NEAR THE GALACTIC CENTER. I. ANALYTIC CONSIDERATIONS

Stephen L. W. McMillan[1] and Simon F. Portegies Zwart[2,3,4]
Received 2002 October 9; accepted 2003 June 13

ABSTRACT

A star cluster in a galactic nucleus sinks toward the galactic center because of dynamical friction. As it spirals inward, the cluster loses mass through stellar evolution, relaxation driven evaporation, and tidal stripping, eventually dissolving in the galactic tidal field. We model the in-spiral of dense young star clusters near the center of our Galaxy to study the extent of the region of parameter space in which the cluster can reach the inner parsec of the Galaxy within a few million years. Since we neglect changes in cluster structure due to internal evolution, the present study is most applicable to star clusters less than about one initial relaxation time old. We find that only star clusters with initial masses $\gtrsim 10^5\ M_\odot$ can reach the Galactic center from an initial distance of $\gtrsim 60$ pc within one initial relaxation time or a few million years, whichever is smaller.

Subject headings: black hole physics — Galaxy: center — Galaxy: nucleus — globular clusters: individual (Arches, Quintuplet) — methods: analytical — stellar dynamics

1. INTRODUCTION

The innermost $\sim$100 pc of the Milky Way Galaxy contains a number of intriguing objects. These include the central $\sim(2\text{–}3) \times 10^6\ M_\odot$ black hole (Genzel et al. 2000; Ghez et al. 2000), a cluster containing at least 15 massive young stars (Tabmlyn & Rieke 1993; Krabbe et al. 1995), a much larger population of older stars (Alexander 1999), and at least two young dense star clusters—the Arches and the Quintuplet systems (Nagata et al. 1995, 1990; Okuda et al. 1990).

Krabbe et al. (1995) found $\sim$15 bright He I emission line stars in the Galactic center. They are part of the comoving 7–8 Myr old $\gtrsim 10^4\ M_\odot$ association known as IRS 16 (Tamblyn & Rieke 1993; Krabbe et al. 1995), and are accompanied by many less luminous stars of spectral types O and B (Genzel et al. 2000). Detailed spectroscopic analysis of the Galactic center region (Najarro et al. 1997) indicate that these emission-line stars are evolved, with a high surface ratio of helium to hydrogen $n_{\rm He}/n_{\rm H} = 1\text{–}1.67$. Allen, Hyland, & Hillier (1990) classify them as Ofpe/WN9 stars, while Najarro et al. (1997) identify them as 60–100 $M_\odot$ luminous blue variables (LBVs), the late evolutionary stages of very massive stars (Langer et al. 1994). Depending on the interpretation of the data, the age of IRS 16 therefore lies in the range 3–7 Myr, the lower figure corresponding to the LBV identification.

One possible explanation for these stars is a recent $\sim 10^4$ $M_\odot$ starburst (Krabbe et al. 1995). However, this model is problematic, as the formation of stars within 1 pc of the Galactic center is difficult; the Galactic tidal field is sufficient to unbind gas clouds with densities $\lesssim 10^7$ cm^{-3} (Güsten & Downes 1980). Gerhard (2001) has proposed that a $10^6\ M_\odot$ star cluster formed at a distance of $\lesssim$30 pc from the Galactic center could have reached the Galactic center via dynamical friction before being disrupted by the Galactic tidal field or by internal dynamical evolution. This qualitative argument solves the problem of the presence of young, very massive stars in the Galactic center. Gerhard's dynamical friction timescale assumed that the stellar density in the vicinity of the Galactic center is described by an isothermal sphere; in addition, he ignored stellar mass loss and the internal dynamical evolution of the cluster. In this paper we present a more quantitative approach to the problem.

This is the first in a series of papers in which we consider the timescale on which a star cluster sinks to the Galactic center and is disrupted by the Galactic tidal field. In the semianalytic calculations presented here, we study the in-spiral of three quite different cluster models. We begin with the simplifying approximation that the in-spiraling object has constant mass. Later, we relax that assumption and allow the cluster to lose mass, first by tidal stripping, then also by stellar evolution and relaxation. For definiteness, and for purposes of illustration, we adopt a simple analytic prescription for mass loss from the evolving cluster, and investigate its consequences. In a future paper we will incorporate more realistic treatments of cluster dynamics.

The organization of this paper is as follows. In § 2 we first consider the orbital decay of a nonevolving point mass. In § 3 we expand our study to include clusters of nonzero radii, allowing their masses to evolve in time as material is stripped by the Galactic tidal field. The introduction of physical parameters into our models then allows us to incorporate simple treatments of stellar mass loss and evaporation within our simple model. In § 4 we apply the model to star clusters near the Galactic center, to determine the region of parameter space in which clusters can transport a considerable fraction of their initial mass to within a few parsecs of the Galactic center before disruption. We discuss our results and conclude in § 5.

[1] Department of Physics, Drexel University, Philadelphia, PA 19104.
[2] Astronomical Institute "Anton Pannekoek," University of Amsterdam, Kruislaan 403, Netherlands.
[3] Institute for Computer Science, University of Amsterdam, Kruislaan 403, Netherlands.
[4] KNAW Fellow.

2. IN-SPIRAL WITH CONSTANT MASS

We begin our study with the simplifying assumption that the mass of the in-spiraling object is constant. This

idealization may be appropriate for a single massive black hole or a very compact star cluster that is much smaller than its Jacobi radius, the limiting radius of a cluster in the tidal field of the Galaxy. In the latter case, however, for the constant-mass approximation to hold, internal dynamical evolution of the cluster should also be negligible on the timescale on which the cluster sinks to the Galactic center. In practice, especially for small clusters, this will not be the case, as we discuss in § 5.

2.1. *Dynamical Friction*

We characterize the mass M within a sphere with radius R centered on the Galactic center as a power law,

$$M(R) = AR^{\alpha} , \tag{1}$$

where A and α are constants, with $1 < \alpha < 2$ of interest here. The density at distance R then is

$$\rho(R) = \frac{A\alpha}{4\pi} R^{\alpha-3} , \tag{2}$$

and we can write expressions for the orbital acceleration at distance R from the Galactic center,

$$a(R) = GAR^{\alpha-2} , \tag{3}$$

the potential

$$\phi(R) = \frac{GA}{\alpha-1} R^{\alpha-1} , \tag{4}$$

the circular velocity

$$v_c^2(R) = GAR^{\alpha-1} , \tag{5}$$

and the total energy of a circular orbit

$$E_c(R) = \frac{1}{2} GAR^{\alpha-1} \left(\frac{\alpha+1}{\alpha-1}\right) . \tag{6}$$

The object's acceleration due to dynamical friction is (Binney & Tremaine 1987, p. 425)

$$\boldsymbol{a}_f = -4\pi \ln\Lambda\, G^2 \rho m \frac{\boldsymbol{v}_c}{v_c^3} \chi . \tag{7}$$

Here, m is the mass of the object, $\boldsymbol{v}_c$ is its velocity vector (in a circular orbit around the Galactic center), $\ln\Lambda \sim \ln\langle r\rangle/R \sim 5$ is the Coulomb logarithm (where $\langle r\rangle$ is the object's characteristic radius, roughly the half-mass radius in the case of a cluster), G is the gravitational constant, and

$$\chi \equiv \mathrm{erf}(X) - \frac{2X}{\sqrt{\pi}} e^{-X^2} , \tag{8}$$

where $X = v_c/\sqrt{2}\sigma$ and $\sigma^2(R)$ is the local one-dimensional velocity dispersion, assumed to be isotropic and locally Maxwellian.

Substitution of equations (1), (2), and (5) into equation (7) results in

$$a_f \equiv |\boldsymbol{a}_f| = \alpha\chi \ln\Lambda \frac{Gm}{R^2} , \tag{9}$$

from which we note that

$$\frac{a_f}{a(R)} = \alpha\chi \ln\Lambda \frac{m}{M} . \tag{10}$$

For $\alpha = 1.2$, we obtain $X \simeq 0.89$ (see Appendix), and hence $\chi \simeq 0.34$. With $\ln\Lambda = 5$ we find $a_f/a(R) \simeq 2m/M$.

2.2. *Orbital Decay*

We can now derive the in-spiral timescale for a star cluster with constant mass m in a power-law density profile given by equation (1). The time derivative of equation (6) is

$$\begin{aligned} \frac{dE_c}{dt} &= \frac{1}{2}(\alpha+1) GAR^{\alpha-2} \frac{dR}{dt} \\ &= -\chi \ln\Lambda\, G^2 \frac{\rho m}{v_c} , \end{aligned} \tag{11}$$

where the second equation expresses the work done by dynamical friction (eq. [9]). Hereafter, R should be interpreted as $R(t)$, the distance from the cluster in question to the Galactic center. Substitution of equations (2) and (5) leads to

$$\frac{dE_c}{dt} = -\alpha\chi \ln\Lambda\, G^{3/2} A^{1/2} m R^{(\alpha-5)/2} , \tag{12}$$

whence

$$\frac{dR}{dt} = -\gamma R^{-(\alpha+1)/2} , \tag{13}$$

where

$$\gamma = 2m \ln\Lambda \frac{\alpha\chi}{\alpha+1} \left(\frac{G}{A}\right)^{1/2} . \tag{14}$$

Solving equation (13) with $R(t) = R_0$ at time $t = 0$ results in

$$R(t) = R_0 \left[1 - \frac{(\alpha+3)\gamma}{2R_0^{(\alpha+3)/2}} t\right]^{2/(\alpha+3)} . \tag{15}$$

Setting $R = 0$ at $t = t_{\rm df}$ and substituting equation (1) yields

$$t_{\rm df} = \frac{\alpha+1}{\alpha(\alpha+3)} \frac{1}{\chi \ln\Lambda} \left(\frac{M_0}{G}\right)^{1/2} \frac{R_0^{3/2}}{m} , \tag{16}$$

where $M_0 = M(R_0)$. In terms of the orbital period of a circular orbit around the Galactic center at distance R_0, $T_0 = 2\pi\left(GM_0/R_0^3\right)^{-1/2}$, equation (16) becomes

$$\frac{t_{\rm df}}{T_0} = \frac{\alpha+1}{2\pi\alpha(\alpha+3)} \frac{1}{\chi \ln\Lambda} \frac{M_0}{m} . \tag{17}$$

For $\alpha = 1.2$, $M_0/m = 10^3$, and $\ln\Lambda = 5$, we find $t_{\rm df} \simeq 40T_0$.

3. CLUSTERS WITH VARIABLE MASS

We now consider the possibility that the mass of the cluster varies with time, $m = m(t)$. Most mass loss from the cluster is the result of tidal stripping as the cluster sinks toward the Galactic center. We begin by determining the Jacobi (tidal) radius $r_{\rm J}$ of the cluster in the tidal field of the Galaxy.

3.1. *Mass of a Tidally Limited Cluster*

The differential acceleration at distance $r_{\rm J}$ from the center of the cluster is obtained from equation (3),

$$\Delta a_{\rm tide} \approx (\alpha-2) GAR^{\alpha-3} r_{\rm J} , \tag{18}$$

or, relative to the internal cluster acceleration at r_J,

$$\frac{|\Delta a_{\rm tide}|}{a_J} = (\alpha - 2)\left(\frac{M}{m_J}\right)\left(\frac{r_J}{R}\right)^3 . \quad (19)$$

Here $a_J = Gm_J/r_J^2$ and m_J, the cluster mass within radius r_J (still to be determined), will henceforth be identified as the cluster mass. Setting $|\Delta a_{\rm tide}| = a_J$, we find

$$\left(\frac{M}{m_J}\right)\left(\frac{r_J}{R}\right)^3 = \frac{1}{2-\alpha} . \quad (20)$$

This may be conveniently (and conventionally) expressed in terms of average densities $\overline{\rho}_J = 3m_J/4\pi r_J^3$ and $\overline{\rho}_G = 3M/4\pi R^3$, as

$$\overline{\rho}_J = (2-\alpha)\overline{\rho}_G . \quad (21)$$

To proceed further, we must make a connection between m_J and r_J. Two particularly simple cluster density profiles lend themselves easily to analytic development:

1. A homogeneous sphere of mass m_0, radius b, and uniform density

$$\rho_0 = \frac{3m_0}{4\pi b^3} . \quad (22)$$

2. A Plummer (1911) model of mass m_0 and scale radius b, with

$$\rho(r) = \rho_0\left(1 + r^2/b^2\right)^{-5/2} , \quad (23)$$

where ρ_0 is again given by equation (22).

Note that in each case we assume *fixed* parameters m_0 and b—that is, we neglect structural changes in the cluster due to dynamical evolution or stellar mass loss. This assumption greatly simplifies the calculation, but clearly is of questionable validity when the internal dynamical timescales are comparable to the in-spiral time (see § 5). In the next subsection we expand our model to allow for the effects of mass loss due to stellar evolution and escaping stars. A more complete treatment of the cluster's structural evolution will be the subject of a future paper.

For the homogeneous sphere (case 1), the desired relation between m_J and r_J is simple:

$$m_J = \begin{cases} m_0(r_J/b)^3 & r_J < b , \\ m_0 & r_J \geq b . \end{cases} \quad (24)$$

No solution to equation (21) exists for $\overline{\rho}_G > \rho_0/(2-\alpha)$, and the cluster is destroyed at Galactocentric radius

$$R_{\rm min} = \left[\frac{m_0}{(2-\alpha)Ab^3}\right]^{1/(\alpha-3)} . \quad (25)$$

Outside $R_{\rm min}$, $r_J > b$ and $m = m_0$. Inside, $r_J = m = m_J = 0$.

For the Plummer model (case 2),

$$\overline{\rho}_J = \rho_0\left(1 + r_J^2/b^2\right)^{-3/2} \quad (26)$$

and again, no solution exists for $R < R_{\rm min}$. Outside $R_{\rm min}$, $r_J(R)$ satisfies

$$1 + \frac{r_J^2}{b^2} = (2-\alpha)^{2/3}\left(\frac{m_0}{M_0}\right)^{2/3}\left(\frac{R_0}{b}\right)^2\left(\frac{R}{R_0}\right)^{2-2\alpha/3} . \quad (27)$$

The mass of the cluster is then given by equation (21),

$$m_J(R) = (2-\alpha)M_0\left(\frac{r_J}{R_0}\right)^3\left(\frac{R}{R_0}\right)^{\alpha-3} . \quad (28)$$

We use this model as the basis for our discussion in the remainder of the paper.

3.2. *Mass Loss from Stellar Evolution*

Many clusters dissolve so quickly that stellar evolution barely affects their mass. However, if the cluster survives for more than a few million years, mass loss from the most massive stars may become important (see McMillan 2003 for a recent review). Recent detailed *N*-body simulations by Portegies Zwart et al. (2001) have quantified the expansion of a tidally limited cluster as its mass decreases. The expansion drives more rapid disruption, while the mass loss slows the in-spiral.

We include stellar mass loss in our model as follows. First we rewrite equation (28) as $m_J(R) = \langle m\rangle n_J(R)$, where $n_J(R)$ is the number of stars within the Jacobi radius and $\langle m\rangle$ is the mean stellar mass, which is now a function of time because of stellar evolution. We assume that the mass functions of the cluster and of the escaping stars are identical. (Again, this is equivalent to the neglect of internal dynamical evolution.) We parameterize the cluster's expansion in response to stellar mass loss by

$$b = b_0\langle m\rangle_0/\langle m\rangle , \quad (29)$$

which is equivalent to the assumption that the cluster loses mass adiabatically, as found by Portegies Zwart et al. (2001).

The mean mass in the cluster can be computed from the initial mass function. For clarity, we assume that all the mass in stars having masses above the cluster's turnoff mass is simply lost from the cluster. So long as the turnoff mass exceeds $\sim 8\ M_\odot$, this assumption is justified by the high-velocity kick imparted to compact objects by the supernovae in which they form, allowing them to escape from the cluster. For older clusters this assumption breaks down as lower mass stars turn into white dwarfs, which do not receive high velocities at formation, although such clusters are not of direct interest in the present paper. Integrating the initial mass function, we find

$$\langle m\rangle = \left(\frac{1-x}{2-x}\right)\frac{m_{\rm to}^{2-x} - m_{\rm min}^{2-x}}{m_{\rm to}^{1-x} - m_{\rm min}^{1-x}} , \quad (30)$$

where x is the exponent for the (assumed) power-law mass function (Salpeter, $x = 2.35$), $m_{\rm to}$ is the cluster turnoff mass, and $m_{\rm min}$ is the lower mass limit. We determine the turnoff mass using fits to the stellar evolution models of Eggleton, Tout, & Fitchet (1989).

3.3. *Mass Loss due to Relaxation*

A tidally limited star cluster in the tidal field of the Galaxy will also lose mass through internal relaxation as occasional interactions between cluster members result in velocities high enough for stars to escape the cluster potential. Portegies Zwart & McMillan (2002) have simulated star clusters near the Galactic center; they derive the following approximate expression for relaxation-driven cluster

mass loss,

$$m(t) = m_0\left(1 - \frac{t}{0.29t_{\rm rt}}\right) . \quad (31)$$

Here $t_{\rm rt}$ is the relaxation time at the cluster tidal radius,

$$t_{\rm rt} = 2.05\ {\rm Myr}\left(\frac{r_{\rm J}}{1\ {\rm pc}}\right)^{3/2}\left(\frac{m_{\rm J}}{M_\odot}\right)^{-1/2}\frac{n_{\rm J}}{\log(0.4n_{\rm J})} , \quad (32)$$

where $n_{\rm J}$ is the number of stars contained within the Jacobi radius.

The clusters in the study of Portegies Zwart & McMillan (2002) did not spiral in to the Galactic center, so the relaxation time at the tidal radius remained constant over the lifetime of the cluster. In our case, where clusters sink toward the Galactic center, the relaxation time at the tidal radius changes with time. We therefore recast equation (31) as follows. Differentiating equation (31) with respect to time, identifying $m(t)$ with $m_{\rm J}$ and $t_{\rm rt}$ with the instantaneous relaxation time at $r_{\rm J}$, and including the radial dependence of the relaxation time, assuming a tidally limited cluster, we obtain

$$\frac{dm}{dt} = -\frac{m_0}{0.29t_{\rm rt,0}}\left(\frac{R}{R_0}\right)^{(\alpha-3)/2} . \quad (33)$$

For the purposes of this paper, we draw a distinction between the processes of *tidal stripping*, in which stars outside the Jacobi radius are removed by the Galactic tidal field as the cluster sinks toward the Galactic center and the Jacobi radius shrinks, and *evaporation*, in which stars are driven across the instantaneous Jacobi radius by internal two-body relaxation. All models discussed in the following section include tidal stripping; models discussed in § 4.2 and subsequently also include both evaporation-driven and stellar-evolution mass loss.

4. RESULTS

From § 2.2, the distance from the cluster to the Galactic center satisfies

$$\frac{dR}{dt} = -\gamma(R)R^{-(\alpha+1)/2} \quad (34)$$

(eqs. [13] and [14]), with $R = R_0$ at $t = 0$. Transforming to dimensionless variables $\xi = R/R_0$ and $\tau = t/T_0$, and substituting equation (14), we rewrite this equation in the form

$$\frac{d\xi}{d\tau} = \frac{4\pi\alpha}{\alpha+1}\chi\ln\Lambda\frac{m_{\rm J}}{M_0}\xi^{-(\alpha+1)/2} . \quad (35)$$

For a Plummer model, the cluster mass $m_{\rm J}$ varies as a function of R and therefore ξ via equation (28). We solve equation (35) numerically, as it admits no simple analytic solution. For all models we adopt $A = 4.25 \times 10^6\ M_\odot$ (measuring R in eq. [1] in parsecs) and $\alpha = 1.2$ (Sanders & Lowinger 1972; Mezger et al. 1999).

For simplicity, we assume that $\chi\ln\Lambda = 1$ for the remainder of this section, unless indicated otherwise. A value of $\chi\log\Lambda = 1.2$ or 1.3 is probably more appropriate (Binney & Tremaine 1987; Spinnato, Fellhauer, & Portegies Zwart 2003). The dynamical friction timescale is inversely proportional to $\chi\ln\Lambda$ (see eq. [16]), so the effects of different choices can be easily estimated.

4.1. *Solutions without Stellar Evolution*

For systems without significant stellar mass loss or evaporation, the evolution can be conveniently parametrized by the dimensionless quantities

$$\beta = b_0/R_0 ,$$
$$\mu = m_0/M_0 . \quad (36)$$

The contours and gray scale in Figure 1 present the scaled cluster lifetime ($t_{\rm diss} \equiv t_{\rm rmd}/T_0$, where $t_{\rm diss}$ is the cluster dissolution time) as a function of β and μ.

Figure 1 shows that compact, massive clusters have the shortest lifetimes, and that the lifetime decreases with increasing mass at fixed initial cluster radius (b_0), increases with increasing radius at fixed mass, and is largely independent of the radius for small radii. This last point simply means that clusters initially well inside their Jacobi radii ($b_0 \ll 0.9r_{\rm J}$) experience significant stripping only near the end of the in-spiral process. There is no initial solution when $\overline{\rho}_G > \rho_0/(2-\alpha)$, i.e. when $b_0 > r_{\rm J}$.

Since the stellar density diverges toward the Galactic center, no extended cluster can actually reach $R = 0$ (although a black hole can). Figure 2 shows the cluster's distance to the Galactic center as a function of time (again in units of the initial orbital period of the cluster around the Galactic center) for several selected values of β and μ. Not surprisingly, more massive clusters (larger values of μ) spiral in more quickly, and physically larger clusters (larger β) dissolve at larger distances from the Galactic center.

The long lifetimes of clusters with $b_0 \gtrsim 0.9r_{\rm J}$ (see Fig. 1) and small values of μ are due to the weak effect of dynamical friction in those cases. Since we ignore stellar mass loss and internal dynamical evolution (specifically, evaporation) in

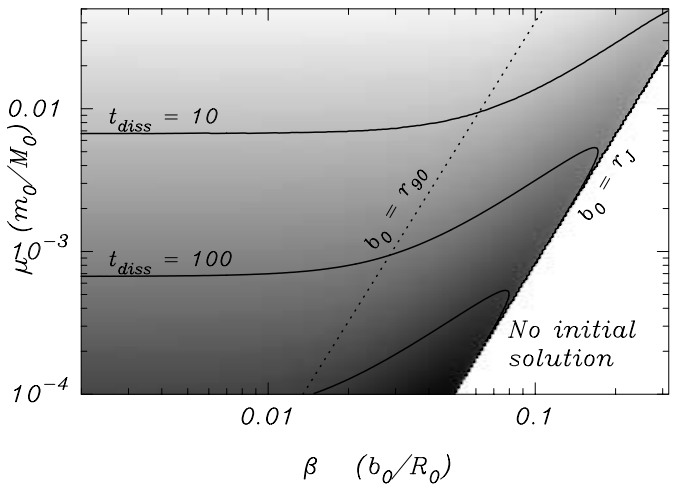

FIG. 1.—Scaled cluster lifetime $t_{\rm diss}$ (*contours and gray scale*) as a function of the dimensionless parameters β and μ (see eqs. [35] and [36]), for models with tidal stripping but without additional mass loss by stellar evolution or evaporation. The parameter β is the ratio of the initial cluster length scale to the initial distance to the Galactic center. The parameter μ is the ratio of the initial cluster mass to the mass of the Galaxy contained within the initial orbit. The numerical labels on the contours give the scaled disruption time $t_{\rm diss}$ in units of the cluster's initial orbital period around the Galactic center. The gray shades provide the same information as the contours; darker shades represent longer cluster lifetime. The dotted line indicates the values of β and μ corresponding to $b_0 = 0.9r_{\rm J}$; the characteristic scale of the initial Plummer model is 90% of the cluster Jacobi radius. No initial solution exists for the area to the right of the curve $b_0 = r_{\rm J}$ (also indicated).

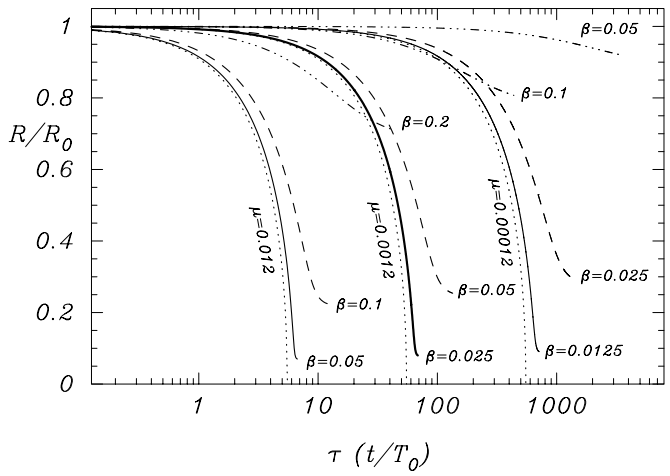

FIG. 2.—Scaled distance to the Galactic center R/R_0 as a function of scaled time t/T_0, for selected combinations of β and μ. The three families of models shown have $\mu = 0.012$ (*left set of curves*), $\mu = 0.0012$ (*middle curves*), and $\mu = 0.00012$ (*rightmost curves*). The dotted lines give the evolution for a constant point mass ($\beta = 0$); other curves present models with β as indicated. The model corresponding to $\mu = 0.0012$, $\beta = 0.025$ (*heavy solid line*) is the basis for Figs. 3–5.

this simple model, such clusters survive for unrealistically long times. In practice, these systems will be strongly affected by stellar evolution and evaporation, as we now demonstrate.

4.2. *Evolution with Stellar Mass Loss and Relaxation*

By selecting the Galactic center as a representative nucleus, we can attach physical units to the selected values of μ and β. The advantage of introducing physical parameters is that the numbers become more intuitive, but of course we lose the scale-free solution from previous section. Another advantage of fixing the scaling is that we can take stellar evolution and internal relaxation into account. Stellar mass loss (via eq. [30]) and evaporation (via eq. [33]) are included by solving equation (35). For most calculations we adopted a Salpeter initial mass function between 0.1 and 100 $M_\odot$. The effect of relaxing this assumption is illustrated in Figure 5 below.

Figure 3 shows distances to the Galactic center as a function of time for model clusters having initial masses of 64,000 $M_\odot$ (Fig. 3*a*) and 256,000 $M_\odot$ (Fig. 3*b*). For each selected initial distance ($R_0 = 2$, 4, 8, and 16 pc) we choose a range of initial values for the cluster scale, $b_0 = 0.2$, 0.4, and 0.8 pc. The choice of $m_0 = 64,000\ M_\odot$, $R_0 = 8$ pc, and $b_0 = 0.2$ pc corresponds to the "standard" model indicated in Figure 2. These models were computed taking both stellar mass loss and evaporation into account. Models with $b_0 = 0$ (point mass case, without stellar mass loss or evaporation) are also included for comparison; they are identical to the calculations presented in Figure 2.

As a result of the extra mass-loss channels (stellar evolution and evaporation) and the resulting reduction in the inspiral (and hence tidal stripping) rate, the lifetimes of the clusters shown in Figure 3 may be either longer or shorter than those of clusters in which stellar evolution is neglected (as in Fig. 2). This is illustrated in Figure 4 for models having $\mu = 0.00012$ and $\beta = 0.05$, 0.025 (the "standard" model), and 0.0125. Dimensionless times are converted to Myr using an orbital period of 0.30 Myr, appropriate to a cluster at an initial distance of 8 pc from the Galactic center. The dotted curves show the evolution of the dimensionless models in which only tidal stripping is included. The solid, dashed, and dash–triple-dotted curves present the same models with stellar evolution and evaporation taken into account. At a distance of 8 pc from the Galactic center, the values of $\beta = 0.05$, 0.025, and 0.0125 correspond to $b_0 = 0.4$, 0.2, and 0.1 pc, respectively.

Compact clusters ($b_0 \lesssim 0.4$ pc) are relatively unaffected by tidal stripping. As a result, the primary effect of stellar mass loss is simply to decrease the in-spiral rate, increasing the cluster lifetime. However, in larger clusters ($b_0 \gtrsim 0.4$ pc) the expansion caused by stellar mass loss greatly increases the stripping rate, significantly decreasing the lifetime despite the slower in-spiral. For very low mass, or very large, clusters, relaxation and evaporation may dominate. However for the cases studied here the effect is almost negligible. This is illustrated by the first few million years of

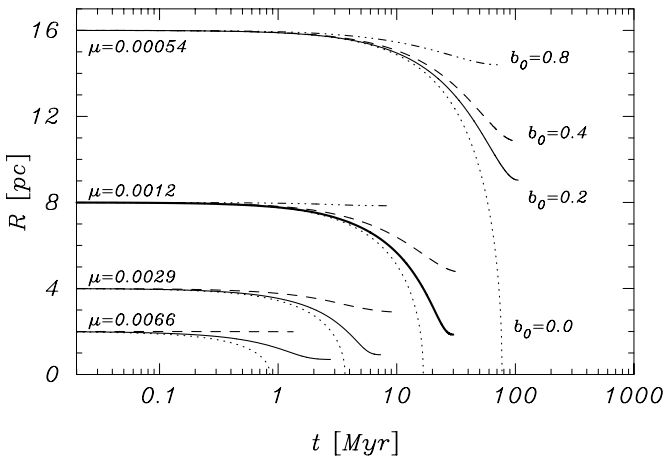

FIG. 3*a*

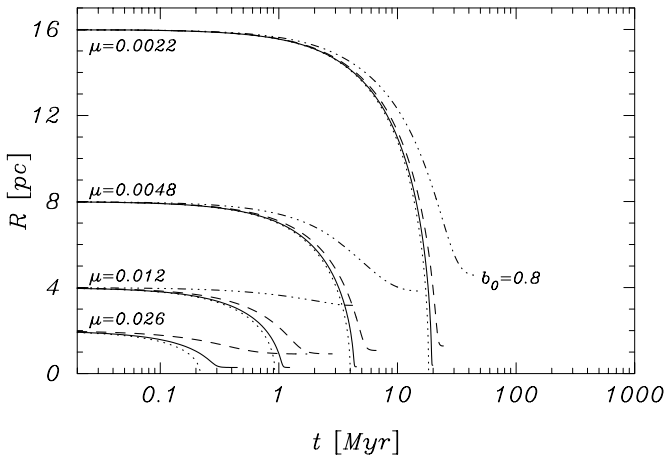

FIG. 3*b*

FIG. 3.—Time evolution of Galactocentric distance R for models with (*a*) $m = 64,000\ M_\odot$ and (*b*) 256,000 $M_\odot$, assuming $\chi \ln \Lambda = 1$. Initial cluster scales b_0 are 0.0 (*dotted lines*), $b = 0.2$ (*solid line*), 0.4 (*dashes*), and 0.8 (*dash-triple-dotted lines*). The corresponding values for μ are indicated near the start of each family of curves. The "standard" model marked in Fig. 2 is also indicated here (*heavy solid line*). For reference, the orbital periods of clusters at 2, 4, 8, and 16 pc from the Galactic center are 0.09, 0.16, 0.30, and 0.56 Myr, respectively.

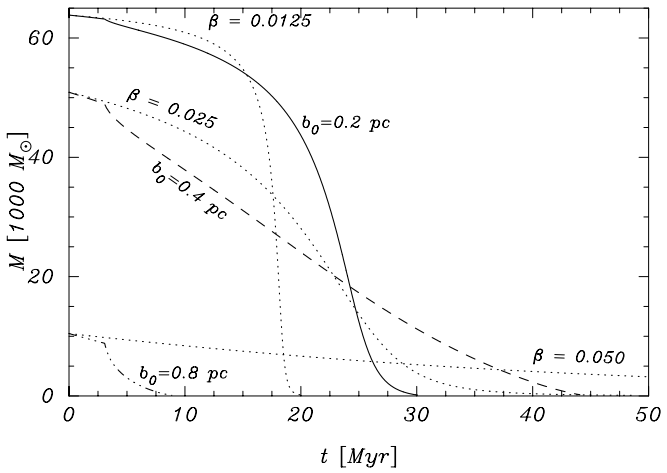

FIG. 4.—Mass as a function of time for a 64,000 $M_\odot$ star cluster at a distance of 8 pc from the Galactic center ($\mu = 0.00012$) with various values for b_0 (as indicated). The dotted curves present the corresponding evolution of the cluster without stellar evolution or evaporation. The values of β correspond to the choices of b_0. All calculations were made using $\chi \ln \Lambda = 1$.

evolution of clusters with large b_0, such as the dash–triple-dotted curve in Figure 4. The small deviation of the $b_0 = 0.8$ pc curve from the $\beta = 0.050$ dotted curve during the first ~5 Myr is the result of relaxation.

Figure 5 illustrates how varying the cluster initial mass function alters the time evolution of its Galactocentric radius and mass. The dotted curve (Fig. 5*a* only) shows the constant point-mass case for $\mu = 0.0012$. The solid curve shows the evolution of the standard model with $\beta = 0.025$, scaling times to Myr assuming an initial Galactocentric distance of 8 pc. The dashed curves give the results when stellar mass loss and evaporation are taken into account, assuming lower mass limits for the initial mass function of 0.1, 0.2, 0.4, and 0.8 $M_\odot$.

Increasing the low-mass cutoff in the mass function increases the effective stellar evolution mass-loss rate, and reduces the cluster lifetime. A similar effect can be achieved by increasing the power-law slope x of the mass function. The models are therefore degenerate in the x-$m_{\rm min}$ plane. For example, a model with a Salpeter initial mass function ($x = 2.35$) and a low-mass cutoff at 0.2 $M_\odot$ evolves almost identically to a model with $x = 2.13$ and $m_{\rm min} = 0.1$ or with $x = 2.90$ and $m_{\rm min} = 0.4$.

4.3. *Comparison with Kim et al. (2000)*

Kim (2000) used GADGET, the tree code developed by Springel, Yoshida, & White (2001), to compute the dynamical friction of dense star clusters near the Galactic center. In these calculations, the inner part of the Galaxy was represented by 2 million point particles distributed as a truncated softened power-law similar to our equation (2), except that the overall density was 2.5 times smaller than ours. The black hole in the Galactic center was represented as a single particle. The star cluster was modeled as a Plummer sphere with $b_0 = 0.85$ pc, using 10^5 point particles having a total mass of $m_0 = 10^6$ $M_\odot$. Initially, the cluster was placed in a circular orbit at a distance of $R_0 = 30$ pc from the Galactic center. The simulations ignored mass loss by stellar evolution and evaporation.

The time dependence of the cluster's Galactocentric distance, as determined by Kim (2000), is shown in Figure 6. His cluster orbits become slightly eccentric during the evolution, but this seems to have little effect on the dynamical friction timescale. For clarity we do not show the actual results reported by Kim, but instead match his initial conditions, which are plotted in Figure 6 as the rightmost dashed curve. This model is computed without stellar evolution or evaporation, as in Kim's simulations. Our model closely reproduces Kim's results when we adopt $\ln \Lambda = 3.7$, which is close to the value used by Kim. For reference, we also plot the evolution of a constant point-mass model (*dotted curve*), and a model in which stellar evolution and evaporation are taken into account (*solid curve*). To guide the eye, we also plot the same series of runs with $\ln \Lambda = 10$.

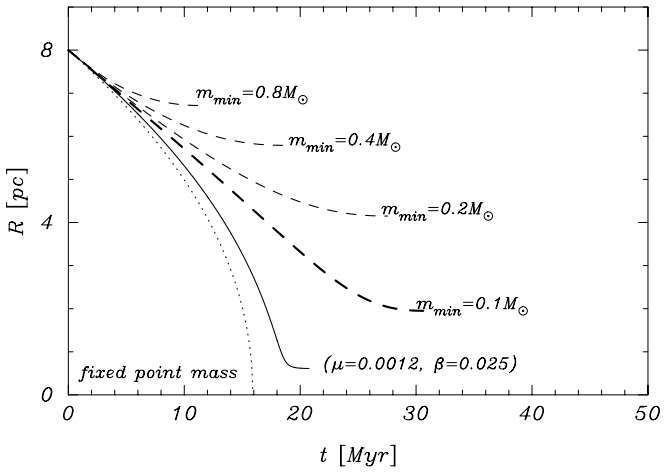

FIG. 5*a*

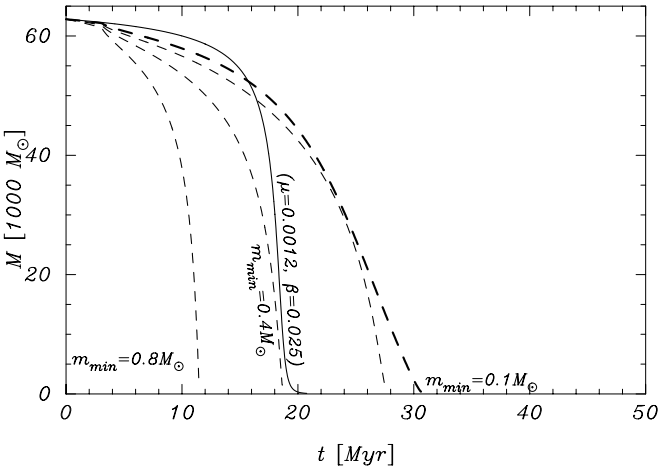

FIG. 5*b*

FIG. 5.—Evolution of (*a*) the distance to the Galactic center and (*b*) mass for model clusters with initial mass $m_0 = 64,000$ $M_\odot$, initial radius $b_0 = 0.2$ pc, and initial Galactocentric distance $R_0 = 8$ pc. The dotted curve in (*a*) shows the evolution of the model without stellar evolution or evaporation, assuming that the cluster is a point mass. The solid curves are the "standard" model, computed without stellar evolution or evaporation, with $\beta = 0.025$, appropriate to the choice of b_0. The dashed curves include stellar evolution and evaporation and are computed using a Salpeter initial mass function with different lower mass limits $m_{\rm min}$, ranging from 0.1 $M_\odot$ (*heavy dashed line*) to 0.8 $M_\odot$ (as indicated). As before, we assume $\chi \ln \Lambda = 1$.

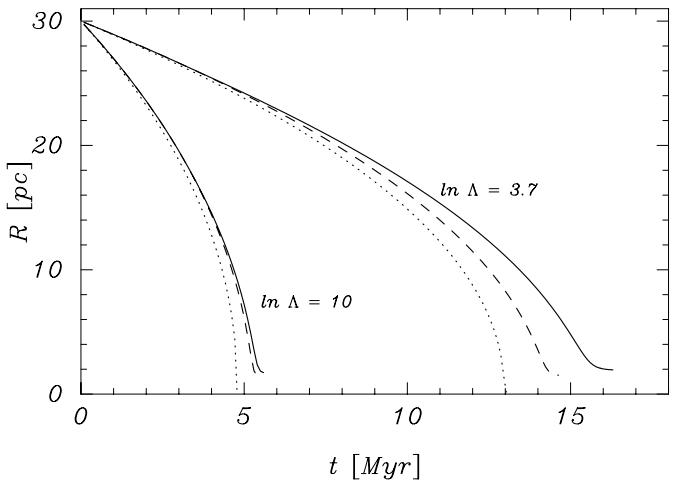

FIG. 6.—Time evolution of Galactocentric distance R of a star cluster having an initial mass $m = 10^6\ M_\odot$. The rightmost set of curves represents model 1 of Kim (2000), and have $\ln\Lambda = 3.7$; the leftmost curves have $\ln\Lambda = 10$. Dotted lines are for a point-mass ($\beta = 0$) cluster with $\mu = 0.00845$. Dashed lines are for models with $b_0 = 0.85$ pc, but excluding stellar evolution and evaporation, as assumed by Kim (2000). Solid curves include stellar mass loss and evaporation, with a Salpeter initial mass function between 0.1 and 100 $M_\odot$. Although Kim (2000) continued his calculation for only about 9 Myr, his curve and our rightmost dashed curve are virtually indistinguishable.

5. DISCUSSION

In this section we discuss some consequences of our semi-analytical calculations. In particular, we consider Gerhard's (2001) conjecture, discussed in § 1, that IRS 16 and the associated young stars observed in the Galactic center may have been deposited there by the in-spiral and disruption of a much more massive system. We take the two known Galactic center clusters—the Arches and Quintuplet—as templates.

Table 1 presents the observed parameters for the Arches and Quintuplet systems. The final columns give the clusters' half-mass relaxation time and the time required to reach the Galactic center, according to equation (32). (The half-mass relaxation time is computed by substituting $r_{\rm hm}$ for $r_{\rm J}$ in that equation.) It is clear that neither cluster will reach the Galactic center within the next few Myr, and that both were probably born at roughly their present distance from the Galactic center. For these calculations we have again adopted $\chi \log\Lambda = 1$.

Figure 7 presents, as a function of initial cluster mass and galactocentric radius, the time taken for a star cluster with $b_0 = 0.2$ pc to reach the Galactic center (Fig. 7*a*), and the distance from the Galactic center at which the cluster dissolves (Fig. 7*b*). Contours and the gray scale represent in-spiral time in Figure 7*a* and dissolution distance in Figure 7*b*. The cluster is deemed to have dissolved when it comes within 1 pc of the Galactic center, or when it has lost 99% of its initial mass. The dotted lines have the same meanings as in Figure 1.

The rightmost dashed line in Figure 7 marks initial conditions for which the in-spiral timescale equals the initial relaxation time. To the right of this curve, the cluster will experience significant internal dynamical evolution before disrupting. Our simple description of the cluster's internal structure is therefore unreliable to the right of this curve, but our expression for the evaporation rate is still valid. The left dashed curve corresponds to an in-spiral timescale of $0.2t_{\rm rh}$, where $t_{\rm rh}$ is the initial relaxation time at the half-mass radius. This is roughly the core-collapse time for a system with a realistic initial mass function in which stellar evolution is relatively unimportant (see Portegies Zwart & McMillan 2002). Clusters with initial conditions to the left of the left dashed curve are thus expected to dissolve in the Galactic tidal field before experiencing core collapse.

During and after core collapse (to the right of the left dashed curve in Fig. 7*a*) the structure of the cluster changes considerably, and our simple prescription for cluster disruption is unlikely to hold. We expect that the structural changes in these clusters will cause their dense cores to survive for longer, and that they will sink slightly closer to the Galactic center than indicated in Figure 7*b* (see Gerhard 2001 and Portegies Zwart, McMillan, & Gerhard 2003 for further discussion). The change in disruption radius is not expected to be great, however, as the residual core masses are small and their in-spiral correspondingly slow at late times.

Figure 7 clearly indicates that the two known nuclear star clusters, the Arches and Quintuplet, will not reach the Galactic center. Their survival times are determined by internal relaxation rather than by dynamical friction (see also Table 1). The in-spiral timescale for these clusters is of the order of 1 Gyr, compared to their predicted lifetime of 100 Myr, based on N-body simulations (Portegies Zwart et al. 2001). Figure 7*b* indicates that clusters with $M \lesssim 20,000\ M_\odot$ barely evolve in Galactocentric radius on this timescale, but instead dissolve in situ, as a result of the combined effects of evaporation and stellar mass loss.

Figure 8 gives the time taken for a star cluster with $m_0 = 64,000\ M_\odot$ to reach the Galactic center and the

TABLE 1
OBSERVED PARAMETERS FOR THE ARCHES AND QUINTUPLET STAR CLUSTERS

Name	Reference	$R_{\rm gc}$ (pc)	Age (Myr)	M ($M_\odot$)	$R_{\rm hm}$ (pc)	$t_{\rm rt}$ (Myr)	$t_{\rm diss}$ (Myr)	$t_{\rm df}$ (Gyr)
Arches.....	1	30	2–4	12–50	0.2	12	60	0.3–1.9
Quintuplet	2, 3, 4	35	3–5	10–16	0.5	12	60	5.5–9.6

NOTES.—Both clusters lie within 35 pc (in projection) of the Galactic center. The first two columns give the cluster name and references, followed by the distance to the Galactic center, age, mass, and half-mass radius. The last three columns give the two-body relaxation time at the half-mass radius, the expected time to disruption, and the in-spiral timescale.

REFERENCES.—(1) Figer et al. 1999a; (2) Glass, Catchpole, & Whitelock 1987; (3) Nagata et al. 1990; (4) Figer, Mclean, & Morris 1999b.

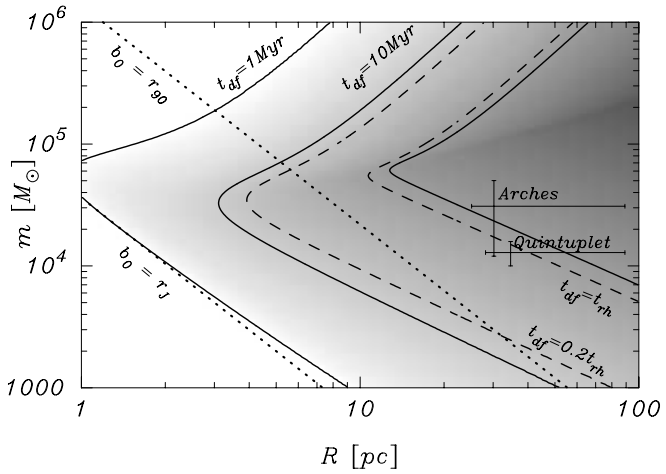

FIG. 7*a*

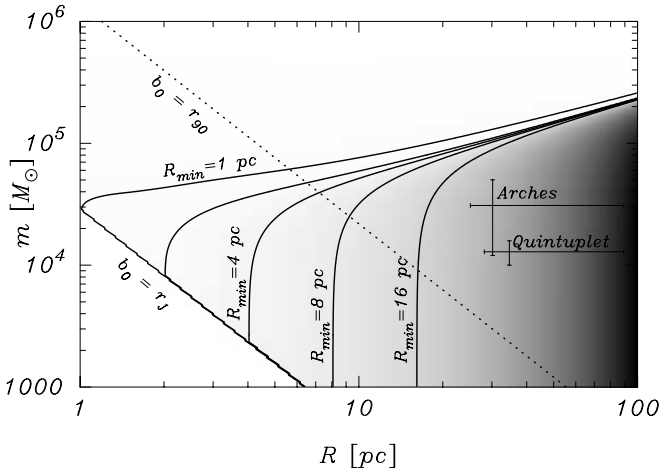

FIG. 7*b*

FIG. 7.—(*a*) In-spiral time and (*b*) final distance to the Galactic center for clusters with $b_0 = 0.2$ pc, as functions of initial galactocentric distance and cluster mass. The dotted lines correspond to $b_0 = 0.9r_J$ and $b_0 = r_J$, as in Fig. 1. The solid curves indicate initial conditions where the dynamical friction in-spiral timescale t_{df} is 1 Myr (*left*), 10 Myr, and 100 Myr (*right*). The dashed curves in panel *a* correspond to $t_{df} = 0.2t_{rh}$ (*left*) and $t_{df} = t_{rh}$ (*right*), where t_{rh} is the initial half-mass relaxation time of the cluster, obtained by substituting r_{hm} for r_J in eq. (32). The approximate locations of the Arches and Quintuplet clusters (see Table 1) are also shown.

Galactocentric distance at which the cluster dissolves. In Figure 7 the initial cluster mass m_0 was varied at constant b_0. Now we vary b_0 keeping m_0 constant, thereby providing a second slice through the same parameter space as in Figure 7. As in Figure 7, the approximate locations of the Arches and Quintuplet clusters are indicated. It is clear that small shifts in either figure will not alter the basic conclusion that both clusters will dissolve at large distances from the Galactic center.

From Figures 7 and 8 it is clear that only massive ($\gtrsim 10^5$ $M_\odot$) star clusters can transport a significant fraction of their mass to the vicinity of the Galactic center within a few Myr. Also, even a 10^6 $M_\odot$ star cluster will require several tens of Myr to reach the Galactic center from an initial distance of $\gtrsim 30$ pc. The most promising candidates to reach the central parsec of the Galaxy within 10 Myr, but after significant mass segregation has occurred, are star clusters with masses $\lesssim 10^5$ $M_\odot$, born within about 20 pc of the Galactic center, with half-mass radii of $\sim$0.2–0.4 pc. Less massive clusters, clusters farther from the Galactic center, or smaller (larger) clusters have greater difficulty reaching the Galactic center before disruption (core collapse).

We therefore conclude that, if they originated in a massive star cluster, the stars in IRS 16 were born in a $\lesssim 10^5$ $M_\odot$ cluster at a Galactocentric distance of $\lesssim 20$ pc. The cluster deposited about 10^3 $M_\odot$ of material within $\sim$3 pc of the Galactic center. Since such a cluster would have experienced core collapse on about the same timescale, the most massive stars had already segregated to the cluster core. The deposited (core) material was therefore rich in massive stars. These findings are contrary to the results reported by Kim (2000).

More detailed studies are underway to qualify and quantify these statements (Portegies Zwart et al. 2003). Preliminary results indicate that the in-spiral times derived here are in good agreement with *N*-body calculations using the

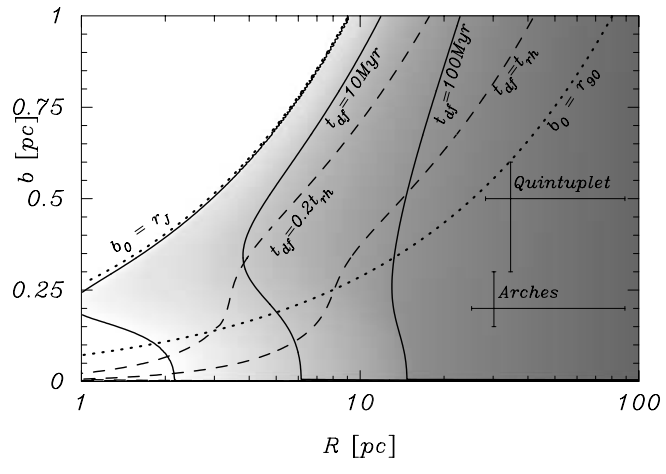

FIG. 8*a*

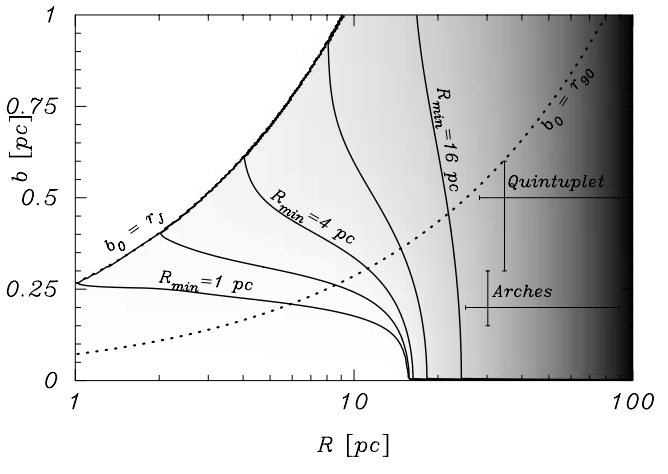

FIG. 8*b*

FIG. 8.—Contours and gray-scale map of (*a*) in-spiral time and (*b*) final distance to the Galactic center for clusters with $m_0 = 64,000$ $M_\odot$, as functions of initial Galactocentric distance R_0 and cluster size b_0. The dashed and dotted curves have the same meanings as in Fig. 7, and the two crosses mark the estimated locations of the Arches and Quintuplet clusters (see Table 1).

GRAPE-6 special-purpose computer (Makino et al 2002), with the same description of dynamical friction as presented here. More sophisticated calibration of the dynamical friction parameters themselves, obtained by modeling the Galactic background as individual stars, will be the subject of a future paper.

We are grateful to Jun Makino and Piet Hut for helpful discussions, and thank the Institute for Advanced Study and Tokyo University for their hospitality and the use of their GRAPE-4 and GRAPE-6 hardware. This work was supported by NASA through Hubble Fellowship grant HF-01112.01-98A awarded by the Space Telescope Science Institute and by NASA ATP grants NAG5-6964 and NAG5-9264, by the Royal Netherlands Academy of Sciences (KNAW), and the Netherlands Research School for Astronomy (NOVA).

APPENDIX

The argument $X = v_c/\sqrt{2}\sigma$ in the dynamical friction relation (eq. [7]) of § 2.1 can be evaluated as follows for in-spiral through a sequence of nearly circular orbits.

Following Binney & Tremaine (1987, eqs. [4]–[30]), we write the equation of dynamical equilibrium (the radial Jeans equation) for stars near the Galactic center as

$$\frac{d}{dR}(\rho\sigma^2) = -\rho\frac{d\phi}{dR} = -\rho\frac{v_c^2}{R} \ , \tag{A1}$$

where we assume an isotropic velocity distribution. In the power-law region, $M \propto R^\alpha$ (eq. [1]), we further assume that $\sigma^2 \propto v_c^2$. It then follows that $\sigma^2\rho \sim R^{2\alpha-4}$, so

$$R\frac{d}{dR}(\sigma^2\rho) = (2\alpha - 4)\sigma^2\rho \ . \tag{A2}$$

Substitution in equation (A1) then yields $X = \sqrt{2-\alpha}$. We note that, as $\alpha \to 1$, this reduces to the correct expression for an isothermal sphere (see Binney & Tremaine 1987, p. 230).

REFERENCES

Alexander, T. 1999, ApJ, 527, 835
Allen, D. A., Hyland, A. R., & Hillier, D. J. 1990, MNRAS, 244, 706
Binney, J., & Tremaine, S. 1987, Galactic Dynamics (Princeton: Princeton Univ. Press), 425
Eggleton, P. P., Tout, C. A., & Fitchett, M. J. 1989, ApJ, 347, 998
Figer, D. F., Kim, S. S., Morris, M., Serabyn, E., Rich, R. M., & McLean, I. S. 1999a, ApJ, 525, 750
Figer, D. F., McLean, I. S., & Morris, M. 1999b, ApJ, 514, 202
Genzel, R., Pichon, C., Eckart, A., Gerhard, O. E., & Ott, T. 2000, MNRAS, 317, 348
Gerhard, O. 2001, ApJ, 546, L39
Ghez, A. M., Morris, M., Becklin, E. E., Tanner, A., & Kremenek, T. 2000, Nature, 407, 349
Glass, I. S., Catchpole, R. M., & Whitelock, P. A. 1987, MNRAS, 227, 373
Güsten, R., & Downes, D. 1980, A&A, 87, 6
Kim, S. S. 2000, BAAS, 197, 409
Krabbe, A., et al. 1995, ApJ, 447, L95
Langer, N., Hamann, W.-R., Lennon, M., Najarro, F., Pauldrach, A. W. A., & Puls, J. 1994, A&A, 290, 819
McMillan, S. L. W. 2003, in Proc. IAU Symp, 208, Astrophysical Supercomputing Using Particle Simulations, ed. J. Makino & P. Hut (San Francisco: ASP), in press
Mezger, P. G., Zylka, R., Philipp, S., & Launhardt, R. 1999, A&A, 348, 457
Nagata, T., Woodward, C. E., Shure, M., & Kobayashi, N. 1995, AJ, 109, 1676
Nagata, T., Woodward, C. E., Shure, M., Pipher, J. L., & Okuda, H. 1990, ApJ, 351, 83
Najarro, F., Krabbe, A., Genzel, R., Lutz, D., Kudritzki, R. P., & Hillier, D. J. 1997, A&A, 325, 700
Okuda, H., Shibai, H., Nakagawa, T., Matsuhara, H., Kobayashi, Y., Kaifu, N., Nagata, T., Gatley, I., & Geballe, T. R. 1990, ApJ, 351, 89
Plummer, H. C. 1911, MNRAS, 71, 460
Portegies Zwart, S. F., Makino, J., McMillan, S. L. W., & Hut, P. 2001, ApJ, 546, L101
Portegies Zwart, S. F., & McMillan, S. L. W. 2002, ApJ, 576, 899
Portegies Zwart, S. F., McMillan, S. L. W., & Gerhard, O. 2003, ApJ, 593, 352
Sanders, R. H., & Lowinger, T. 1972, AJ, 77, 292
Spinnato, P., Fellhauer, M., & Portegies Zwart, S.F. 2003, MNRAS, 344, 22
Springel, V., Yoshida, N., & White, S. D. M. 2001, NewA, 6, 79
Tamblyn, P., & Rieke, G. H. 1993, ApJ, 414, 573